Title: The polarity factor Bucky ball associates with the centrosome and promotes microtubule rearrangements to establish the oocyte axis in zebrafish.

Meredyth M. Forbes[1], Bruce W. Draper[2], and Florence L. Marlow[1,3]

[1] Department of Developmental and Molecular Biology, Albert Einstein College of Medicine of Yeshiva University, Bronx, NY

[2] Department of Molecular and Cellular Biology, University of California Davis, Davis, CA

[3] Department of Neuroscience, Albert Einstein College of Medicine of Yeshiva University, Bronx, NY

*Corresponding Author:

F. L. Marlow (florence.marlow@einstein.yu.edu; 1718-430-4208).

Department of Developmental and Molecular Biology, Department of Neuroscience. Albert Einstein College of Medicine. Yeshiva University. Bronx (NY, USA). 1300 Morris Park Av. 1301, Bronx

Keywords

Bucky ball, oocyte polarity, microtubule organizer, meiosis, *vasa, magellan*

Summary

Cell polarity is a conserved feature of eukaryotic cells that relies on establishment and maintenance of intracellular asymmetries. Primary oocytes of all animals examined contain an evolutionarily conserved structure known as the Balbiani body (Bb), one of the earliest known asymmetries in oocytes. Despite its conserved nature little is understood about the molecular and cellular events that polarize vertebrate oocytes. The vertebrate specific *bucky ball (buc)* is the only gene known to be required for Bb assembly. We have previously shown that Buc protein is an indicator of polarity at zygotene stage, before Bb formation. To determine when oocyte polarity is established we examined Buc and the cytoskeleton at earlier stages of meiosis and in mitotic oogonia, also known as cystocytes. Buc is present in midstage cystocytes and prior to zygotene stage Buc is recruited to the centrosome in a cell cycle independent of meiotic progression. Dynamic microtubules are enriched around the centrosome in pre-Bb oocytes, revealing that these cells are polarized. This early microtubule enrichment is normal when *buc* is disrupted, but at later stages functional Buc or Buc-associated activity is required for robust MT organization. Consistent with a role for Buc in generating these cytoskeletal asymmetries, we detected asymmetric perinuclear EB3 foci, which are indicative of polarized microtubules that form proximal to the centrosome in a Buc-dependent manner. Taken together our results indicate that establishment of polarity begins with the centrosome in mitotic cystocytes and that meiotic microtubule organizer activity requires centrosomal localization of Buc to promote oocyte polarity in zebrafish oocytes.

Introduction

In many animals, including zebrafish, pre-meiotic oocyte precursors called oogonia divide mitotically to form germline cysts (GlCs) comprised of cystocytes that are connected by intracellular bridges (Gondos, 1973; Huynh and St Johnston, 2004; Kloc et al., 2004; Marlow and Mullins, 2008). In most organisms examined, GlCs arise from a single cyst progenitor or cystoblast that undergoes synchronous division with incomplete cytokinesis (Huynh and St Johnston, 2004; Kloc et al., 2004; Pepling et al., 1999). Throughout GlC development, cystocytes share cytoplasm via intercellular bridges called ring canals. Glc development in *Drosophila* has been well characterized. The GlC arises from a single cystoblast that yields a 16-cell cyst (Huynh and St Johnston, 2004; Kloc et al., 2004; Pepling et al., 1999). Proper cyst development and oocyte specification depends on a membrane-skeletal organelle, the fusome, which forms via a branching mechanism (de Cuevas and Spradling, 1998; Deng and Lin, 1997; Huynh and St Johnston, 2004; Kloc et al., 2004; Lin et al., 1994; Marlow and Mullins, 2008; Pepling et al., 1999; Roper and Brown, 2004; Snapp et al., 2004). The fusome maintains synchronous cystocyte divisions and functions in specification of a single oocyte among the 16 cyst cells (de Cuevas and Spradling, 1998; Deng and Lin, 1997; Lin and Spradling, 1995). The fusome serves as a scaffold to generate microtubule asymmetries that facilitate directed trafficking of proteins and mitochondria to the oocyte (Cox and Spradling, 2003; Grieder et al., 2000; Marlow and Mullins, 2008; Roper and Brown, 2004; Snapp et al., 2004). Although a fusome-like structure was described in *Xenopus laevis* GlCs, there is no oocyte selection process as all cystocytes differentiate into oocytes (Kloc et al., 2004) thus, it is not known if the *Xenopus* fusome facilitates directional trafficking in GlCs. However, since the *Xenopus* fusome has a rich network of microtubules with associated centrioles, it has been implicated in positioning precursors for Balbiani body (Bb) formation in oocytes (Kloc et al., 2004).

Although the Bb is a widely appreciated indicator of polarity in animal oocytes, how it forms and when polarity is established in vertebrates are not known. Several lines of evidence suggest that polarization might occur in pre-Bb oocytes. First, analysis of pre-meiotic GlCs of flies, frogs and mice indicate that these early stages are at least transiently polarized relative to their cytoplasmic bridges (Deng and Lin, 1997; Huynh

and St Johnston, 2004; Kloc et al., 2004; Kloc et al., 2008). Second, Buc protein, an essential polarity regulator (Bontems et al., 2009; Marlow and Mullins, 2008), is asymmetrical in zygotene oocytes, before Bb formation (Heim et al., 2014). Finally, *buc* transcripts are present in juvenile zebrafish during early stages of sexual differentiation (Heim et al., 2014) when the early ovary contains mitotic germ cells (GCs) and oocytes in early meiosis (Hartung et al., 2014; Leu and Draper, 2010; Maack and Steinner, 2003; Selman et al., 1993; Takahashi, 1977; Wang et al., 2007)

The centrosome has long been appreciated as a cellular organizing center with microtubule organizing activity in oogonia (cyst stages) and early oocytes (Gard, 1991; Gard et al., 1995; Januschke et al., 2006; Mahowald and Strassheim, 1970; Zhao et al., 2012), that mediates asymmetric segregation of patterning molecules during asymmetric cellular divisions [reviewed in (Yamashita, 2009)]. Failed migration of centrioles in *Drosophila* germline cysts disrupts oocyte specification (Roper and Brown, 2004). Ultrastructural analysis of oocytes in model systems including frogs (Kloc et al., 2004), mice (Kloc et al., 2008), flies (Grieder et al., 2000; Megraw and Kaufman, 2000), fish (Marlow and Mullins, 2008), and human oogonia (Sathananthan et al., 2000) revealed conserved positioning of the centrioles proximal to the cytoplasmic bridges that connect cystocytes. Furthermore, analysis of frog and human GlCs indicates that nuage and eventual Bb components encircle the oogonial centrosome (Kloc et al., 2004) [reviewed in (Sathananthan et al., 2000)]. This conserved architecture has generated models whereby the cytoplasmic bridges function as sites of Bb precursor material accumulation (Huynh, 2006; Kloc et al., 2004). Accordingly, mitotic polarity would establish later meiotic polarity, including the site of Bb formation.

Centrosomes also coordinate chromosomal arrangements during the leptotene-zygotene transition of prophase I (Scherthan et al., 2000), the period when Buc protein is asymmetric (Heim et al., 2014). Previous studies in plants and animals have revealed conserved alignment of meiotic polarity to cellular polarity in plants, which lack centrosomes (Cowan et al., 2001, 2002), or to the centrosomes in animal cells, including zebrafish male GCs (Saito et al., 2014). Conservation of these relationships has generated hypotheses regarding potential coordination or interdependence of cellular and meiotic asymmetries. In one model centromere function is mediated by

diffusible factors emanating from the telomeres that are attached to the nuclear membrane; whereas, another posits that coordination is achieved via physical connection between the telomeres and the centrosome, the telocentrosome [reviewed in (Yoshida et al., 2013)]. Importantly, whether meiotic polarity and oocyte polarization are coincident events or are functionally coordinated in vertebrates is unclear.

Here, we examined pre-meiotic oogonia and oocytes during prophase I of meiosis through establishment of the oocyte animal-vegetal axis marked by the Bb. We show that Buc is present in oogonia and localizes to the centrosome before zygotene stage. Examination of meiosis mutants provides evidence that Buc can polarize before the leptotene-zygotene transition, and reveals a requirement for Vasa, which is required for meiotic progression, to prevent Buc association with the centrosome during mitotic stages. Thus, establishment of Buc polarity occurs independent of meiotic progression. We detected enrichment of dynamic microtubules around the centrosome in pre-Bb oocytes, revealing that these cells polarize via a mechanism that does not require *buc*. However, at later stages functional Buc or Bb-associated activity is required for robust MT organization. Consistent with Buc contribution to generating these cytoskeletal asymmetries, we show that a marker of polarized microtubules accumulates in foci proximal to the centrosome in a Buc-dependent manner. Taken together our results indicate that establishment of polarity begins with the centrosome in mitotic GlCs and that microtubule organizer activity requires centrosomal localization of Buc to promote oocyte polarity in zebrafish.

Results

buc functions prior to Balbiani body formation in pre-meiotic germ cells

Based *buc* transcripts are present in pre-meiotic oocyte precursors we examined Buc protein using BucN antibody (Heim et al., 2014), to investigate whether Buc protein was present and thus might act at these stages to establish oocyte polarity. To select for juvenile ovaries, we exploited the female-specific expression of a *buc* reporter transgene, Tg[*buc*:mApple;cmlc2:mCherry] (Heim et al., 2014). We found that Buc protein was produced in cysts containing two or more cells but was not asymmetrically localized in oogonia (Figure 1A, 6A). The presence of Buc protein in midstage cysts indicates that Buc could act prior to Bb formation and that oocyte polarization may begin in oogonia (Figure 1A).

To investigate potential Buc functions in oogonia, we examined GlCs of WT and *buc* mutants. Although intercellular bridges are present and synaptonemal complexes are present in *buc* mutants (Marlow and Mullins, 2008), *buc* mutant cysts appeared larger or disorganized compared to WT (Figure 2A). To address whether loss of *buc* affected cyst size, we labeled GCs using a transgene that expresses membrane targeted GFP in GCs, Tg[*ziwi*:eGFP CAAX]^{uc11}, counterstained with DAPI, and counted oogonia in GlCs of WT and *buc* mutants (Figure 2B). Oogonia were identified based on morphological features previously described in (Leu and Draper, 2010). We found that WT cysts ranged from 1-16 cells as expected if cystocyte divisions and organization were conserved (de Cuevas et al., 1997; Kloc et al., 2004; Pepling et al., 1999). In contrast, *buc* mutant cysts ranged from 1-24 cells (Figure 2D), indicating that Buc may be required to limit cell divisions, or for proper cyst organization or dissolution. To further investigate potential Buc functions in cystocytes, we analyzed cyst size in Tg[*buc*:cbuc] juvenile ovaries, herein referred to as *cbuc*, which ectopically express Buc and disrupt oocyte polarity (Heim et al., 2014). Similar to *buc* mutants, *cbuc* cysts were irregularly sized (Figure 2D). These results suggest that proper Buc regulation is required for normal cyst development.

In zebrafish the subcellular organization of the GlC has not been reported and whether cysts have a fusome-like structure is not known. Therefore, we examined known fusome markers F-actin and Spectrin (Kloc et al., 2004; Lin et al., 1994), in

zebrafish juvenile ovaries (Figure S1). Although F-actin and Spectrin were present at cellular membranes, we could not detect a prominent fusome-like structure in WT or in *buc* oocytes, which resembled WT (Figure S1A-D). Although we cannot exclude existence of a fusome-like structure, localization of F-actin and Spectrin occurs independent of Buc. Interestingly, Spectrin localized to perinuclear granules in oogonia (Figure S1C,D), where the Vasa containing germ granules are found in oogonia (Draper, 2012) and embryonic PGCs (Knaut et al., 2000; Strasser et al., 2008). These data suggest that zebrafish GlCs may be similar to mouse GlCs, which also lack a prominent fusome-like structure as indicated by EM and marker analysis (Klo et al., 2008; Pepling and Spradling, 1998).

Next, we examined microtubules, as microtubule filaments (MF) are known to traverse the intercellular bridges between cystocytes in flies (Grieder et al., 2000; Lin et al., 1994). Most cells types have two populations of microtubules, dynamic microtubules and stable microtubules, the latter of which are marked by acetylation of α-tubulin [reviewed in (Song and Brady, 2015)]. In WT oogonia, acetylated MFs were sparse and were not asymmetrically distributed (Figure 3A). Stable microtubules in oogonia of *buc* mutants and *cbuc* transgenics resembled WT, suggesting that Buc is dispensable for stable microtubule formation at these mitotic stages (Figure 3C,D). In contrast to stable MFs marked by acetylated tubulin, filaments labeled with α-tubulin formed two distribution classes in WT oogonia (Figure 3E). In the first and most frequently observed (class I, Figure 3E), the nucleus was centrally positioned and microtubules were distributed radially around the nucleus. This localization was predominant in midstage cysts (83%) and primary oogonia (37%). In the second and less frequently observed type (class II, Figure 3E), the nucleus was offset from center and the microtubules were asymmetrically enriched within the cell. In contrast to class I localization, class II was more frequent in primary oogonia (63% observed) and rarely in midstage cysts (2% observed). This microtubule enrichment could be random due to constraints imparted by the asymmetrically positioned nucleus, such that the microtubules passively assemble in regions devoid of the nucleus. Alternatively, this asymmetry could result from a functional centrosome nucleating microtubules that then displace the nucleus. Therefore, we investigated the relationship between nuclear position and the

centrosome by examining ɣ-tubulin, a conserved centrosomes component (Stearns et al., 1991) (Figure 3H-J). In WT oogonia with central nuclei (class I) the centrosomes were adjacent to the oogonial nuclei and proximal to adjacent cystocytes (Figure 3H). Ultrastructural analysis of WT, *buc* mutants, and *cbuc* transgenic oogonia revealed that centrioles were found adjacent to the nucleus and proximal to the intercellular bridge (Figure 3K-M). These results suggest that centrosomes are oriented near the intercellular bridges, and thus oogonia are polarized along the cell division plane in GlCs (Figure 3H-J). In oogonia with asymmetric nuclei (class II), centrosomes were positioned where cytoplasm was most abundant, indicating that the centrosome may be nucleating microtubules and displacing the nucleus.

Next we examined oogonia of *buc* mutants and *cbuc* transgenic females to determine if the microtubule and centrosome asymmetries observed in WT depend on Buc function. We found no differences in acetylated tubulin between WT (Figure 3B), *buc*$^{p43/p43}$ (Figure 3C) and *cbuc* cystocytes (Figure 3D). Like WT, two classes of α-tubulin were observed in *buc* mutants and *cbuc* transgenics and the distribution of each class was of similar frequencies for *buc* mutants (Figure 3F) and *cbuc* transgenics (Figure 4G). Furthermore, the centrosome distribution in *buc* mutants (Figure 3I,K) and *cbuc* transgenics (Figure 3J,L) was comparable to WT. Unexpectedly, microtubules labeled with α-tubulin were sparse in these cystocytes (Figure 3F,G). Taken together these findings revealed asymmetric microtubule organization in WT cystocytes; however, since these asymmetries were intact in *buc* loss-of-function and overexpression contexts, we conclude that transient polarization of the nucleus and of α-tubulin labeled microtubules in cystocytes occurs independent of Buc.

Mitochondria are a major Bb component in primary oocytes. In GlCs of flies, stable microtubules of the fusome are required to transport mitochondria to the Bb of the oocyte (Roper and Brown, 2004) via a mechanism that involves plus-end motor adaptor proteins (Cox and Spradling, 2003). In *Xenopus* oogonia, most examined have been described to have a “juxtanuclear” aggregate that is enriched with mitochondria (al-Mukhtar and Webb, 1971). Moreover, these aggregates are thought to represent Bb precursors. To investigate whether mitochondria in zebrafish oogonia might similarly be asymmetrically distributed, we examined mitochondria distribution in *buc* mutant and

cbuc transgenic GlCs. Ultrastructural analysis showed abundant mitochondria in the cytoplasm of all genotypes examined (Figure 4A-D). Fewer mitochondria were observed in *buc* mutants; however, it was unclear if this reflected reduced numbers or reduced enrichment of mitochondria in the plane of section. We then quantified the distribution of mitochondria (Figure 4E,S2), and found that in most WT (Figure 4A,E) *buc* mutant (Figure 4B,E), and *cbuc* transgenic oogonia (Figure 4C,E), mitochondria were asymmetrically distributed on one side of the nucleus. These observations indicate that asymmetries in mitochondria distribution in oogonia are *buc* independent.

Centrosomes predict Buc localization in zygotene stage oocytes.

If the centrosome is a Bb organizer, then it might mark or determine the site of Bb formation, in which case the centrosome should colocalize with asymmetric Buc protein before Bb assembly at zygotene stage (Heim et al., 2014) or earlier. To address this model we used γ-tubulin to label centrosomes and Buc protein at stages before and after Bb formation. In WT zebrafish oocytes, the centrosome is detectable in St Ia from zygotene-diplotene of prophase I, but is then disassembled or eliminated by St Ib (Li-Villarreal et al., 2015). As predicted by this model, the centrosome colocalized with early asymmetric Buc protein in stage Ia oocytes (Figure 5A), and by stage Ib Buc persisted although the centrosome was absent in WT oocytes (Figure S3A). Colocalization of the centrosome with Buc could indicate that the centrosome recruits Buc protein to nucleate Bb assembly, which once formed may replace centrosomal functions thereafter since centrosomes are present in oogonia (before Buc protein is asymmetric) and in St Ia oocytes when Buc becomes asymmetrically localized (Figure 5A), but are eliminated after the Bb forms (Figure S3A,F). Alternatively, the centrosomes may translocate to the site of asymmetric Buc and future Bb formation. Either way, the centrosomes should be intact in *buc* mutant oocytes before the Bb forms and may be disrupted thereafter. As expected, centrosomes were present in St Ia *buc* oocytes although no Buc protein localized there (Figure 5B,F), and as in WT centrosomes were no longer detectable at stage Ib (Figure S3B,D). This is consistent with our findings in juvenile cysts that *buc* is not required for centrosome localization.

Localization of Buc protein to the centrosomes of WT and normal centrosome dispersal in *buc* mutants, which do not form Bbs raises the interesting possibility that formation of a functional Bb requires assembly of Buc complexes at the centrosome. Previously, we showed that *cbuc* transgenes cause ectopic formation of small Bbs that fail to undergo expansion and translocation to specify the vegetal cortex (Hahn et al., 2014). Thus it is possible that failure to establish animal-vegetal polarity in *cbuc* transgenics might be due to accumulation of Buc protein at extracentrosomal sites. Therefore we examined centrosomes and Buc in *cbuc* transgenic ovaries. Although single γ-tubulin foci were present in *cbuc* stage Ia oocytes (Figure S3C,D) and dispersed by stage Ib (Figure S3C,D), indicating that ectopic Buc does not grossly disrupt centrosome integrity, three classes of Buc localization were observed in *cbuc* primary oocytes (Figure 5C-F). Class I resembled WT oocytes with a Buc aggregate colocalized with the centrosome (Figure 5C). Class II resembled *buc* mutants (Figure 6D), and class III had multiple Buc foci that were not colocalized with the centrosome (Figure 6E). Taken together, these results indicate that the transient centrosome is the site of Buc and Bb assembly in primary oocytes and that Buc complex assembly at centrosomes is essential for oocyte polarity.

Buc localizes to the centrosome in meiotic mutants

Although *buc* mutants disrupt Bb formation, which results in failure to specify the animal-vegetal axis, Buc is dispensable for meiotic progression, including synaptonemal complex formation and eventual polar body extrusion(Marlow and Mullins, 2008). Vasa encodes a conserved RNA helicase essential to germline development and involved in translational control (Carrera et al., 2000; Johnstone et al., 2005; Johnstone and Lasko, 2004; Liang et al., 2003), piRNA biogenesis (Kuramochi-Miyagawa et al., 2010; Lim et al., 2013; Pek and Kai, 2011), in cell cycle control during mitotic stem cell divisions in sea urchin and flies (Pek and Kai, 2011; Tanaka et al., 2000; Yajima and Wessel, 2011), and in *Drosophila* promotes meiotic progression (Ghabrial and Schupbach, 1999), oocyte differentiation and other aspects of GIC development (Styhler et al., 1998). In zebrafish *vasa* is required for progression through prophase I of meiosis (Hartung et al., 2014). To examine establishment of Buc asymmetry and animal-vegetal polarity in the context of impaired meiosis, we examined the centrosome and Buc protein in *vasa*

mutants. To distinguish germ cells from the somatic cells of the gonad, we utilized the *ziwi* promoter reporter transgene, Tg[ziwi:GFP] (Leu and Draper, 2010). In oogonia, Buc was distributed throughout the cytoplasm of WT (Figure 6A), but colocalized with the centrosome in *vasa* mutants (Figure 6B), indicating that asymmetric accumulation of Buc can be uncoupled from meiotic asymmetries at the leptotene-zygotene transition (Figure 6).

Buc is dispensable for centrosome microtubule organization activity before Balbiani body stages but promotes robust microtubule assembly thereafter

Since centrosomes were present in GlCs and aligned with Buc protein in oocytes of WT, but not *buc* and *cbuc* females (Figure 5), we investigated whether centrosome function as a microtubule-organizing center (MTOC) requires Buc (Figure 7). We examined the MF organization of *buc* mutants and transgenics that disrupt polarity in zygotene stage Ia oocytes when the centrosome and Buc colocalize. In WT, MFs were enriched in the cytoplasm where asymmetric Buc was localized, consistent with a functional MTOC in this region (Figure 7A). In *buc* mutants and *cbuc* oocytes MFs were also asymmetrically enriched in the cytoplasm, but their fluorescence intensity appeared reduced compared to WT (Figure 7B,C). Interestingly, we observed an increased network of stable microtubules marked with acetylated tubulin in WT as St Ia progressed (Figure 7D); however, in St Ia oocytes of *buc* mutants and *cbuc* transgenics, this increase was not observed and the stable microtubules appeared to be shorter (Figure 7D). Our analysis of dynamic and stable microtubule populations indicates that both loss-of-Buc of excess-of-Buc may impair centrosome function. Moreover, Buc is not required to assemble MTs before Bb assembly, but Buc or Bb function is required for robust MT assembly and/or stability thereafter.

Localization of the microtubule + end binding protein EB3 depends on Buc

To further investigate MF orientation in oocytes, we generated stable transgenic lines expressing microtubule +TIP marker EB3 (Komarova et al., 2005; Nakagawa et al., 2000; Stepanova et al., 2003) using the germline specific *ziwi* promoter (Leu and Draper, 2010). We examined Tg[*ziwi*:hsa.EB3-mCherry] to visualize the growing tips of the microtubules in WT and mutants. We observed two EB3-mCherry foci flanking the

centrosome and asymmetric Buc protein in WT (Figure 8A-C). These EB3-mCherry foci persisted after centrosome elimination and Bb replacement in WT and were reminiscent of growing microtubules, marked by EB1-GFP foci previously associated with nuclear translocation via microtubule-mediated pushing in *Drosophila* oocytes (Zhao et al., 2012). In *Drosophila* oocytes, nuclear movement contributes to polarizing the anterior-posterior and the dorsal-ventral embryonic axes (Gonzalez-Reyes et al., 1995; Roth et al., 1995). Proximity of EB3 foci to the centrosome and Buc raised the possibility that these foci may be coordinated by Buc and the Bb, or conversely that they may coordinate recruitment of Buc and translocation of the Bb from the nucleus. First, we measured the angle and distances between these foci to the centrosome and to the nucleus to investigate how their spatial organization changes when the centrosome is present during Bb assembly (20-40μm oocytes) and after centrosome loss during Bb growth and translocation (40-60μm oocytes) (Figure 8D-I). We found that foci position relative to the MTOC, or later, to the growing Bb was maintained as the Bb moved toward the vegetal cortex, consistent with coordinated organization of these subcellular structures and the nucleus.

Next we asked if the EB3 foci were coordinating polarity either by mediating cues from the nucleus or the centrosome, or alternatively if Buc or the Bb might coordinate EB3 foci. To distinguish between these possibilities we crossed the EB3 transgene into zebrafish *buc* (Bontems et al., 2009) and *mgn* (Dosch et al., 2004; Gupta et al., 2010) polarity mutants and *cbuc* transgenic backgrounds. If the nucleus or centrosome provides a coordinating cue then EB3 foci should be present in *buc* mutants when the centrosome is present, and should be impaired in *mgn* mutants, which disrupt nuclear position (Gupta et al., 2010). If Buc or the Bb provides the coordinating cue, then EB3 foci should be absent or mislocalized in *buc* mutants and *cbuc* transgenics, and show a distorted arrangement due to the abnormally large Bb of *mgn* mutants (Gupta et al., 2010). Consistent with involvement of Buc or a Bb cue, EB3 foci were rarely detected in *buc* mutants and when present only a single EB3 aggregate was observed in 20-40μm oocytes (Figure 9A,C). Notably, in *cbuc* transgenic oocytes EB3 foci failed to form (Figure 9C), which further supports the notion the alignment of Buc protein and the centrosome is essential for oocyte polarization. Moreover, in *mgn* mutants the geometry

of EB3 foci relative to the asymmetric nucleus and the Bb was diamond shaped and comparable to the arrangement in WT at early stages (Figure 9D), but later became triangular as the distance between foci increased during Bb translocation in WT (Figure 8B, 9B,D). Interestingly, at later stages once the centrosome disappeared and the Buc domain moves away from the nucleus, the distance between EB3 foci was greater in *mgn* mutants compared to WT 48.4 µm ± .8 and 29.4 µm ± .8. These results indicate that Buc or the Bb is required for the formation and positioning of these EB3 centers.

Discussion

Our study characterizes early pre-meiotic stages and early meiotic stages of oocyte development in zebrafish to identify cellular asymmetries and their relationship to the Bb precursor Buc. Here, we find that Buc protein is produced in cystocytes, indicating oocyte polarization may be initiated before early asymmetric Buc localization at zygotene stage. We show that Buc first localizes to the centrosome that was present in GlCs. Moreover, Buc-centrosome colocalization can occur independent of meiotic progression, and Vasa prevents Buc recruitment in oogonia. Although assembly of Buc aggregates does not require centrosome colocalization, Buc alignment with the centrosome is required for robust MFs in primary oocytes during Bb assembly. Finally, we show that Buc dependent foci of growing microtubules are first detected in meiotic stages adjacent to the centrosome and the Buc domain, and then after centrosome disassembly associate with the Bb, where Buc is localized. Cumulatively, our results indicate that polarity establishment begins with the centrosome in cyst cells and that microtubule organizer activity requires centrosomal localization of Buc to promote oocyte polarity in zebrafish.

Germline cyst asymmetries are independent of Buc

While Buc is the earliest asymmetric marker in oocytes, it is not known whether polarity is established prior to Buc localization. To address this possibility, we examined female GlCs, which contain mitotic oocyte precursors. Our characterization and prior examination of GlC development indicates that zebrafish GlCs arise from synchronous cell divisions like in other organisms (de Cuevas et al., 1997; Kloc et al., 2004; Marlow and Mullins, 2008; Nakamura et al., 2010; Pepling and Spradling, 1998). We found that Buc protein is produced but not asymmetrically localized in cystocytes, which suggests that Buc later localizes along an uncharacterized axis of polarity that normally forms concomitant with, but, as shown by *vasa* mutants, is not dependent on meiotic progression. Several studies indicate that a fusome polarizes germline cysts of flies and frogs (Cox and Spradling, 2003; de Cuevas and Spradling, 1998; Deng and Lin, 1997; Grieder et al., 2000; Kloc et al., 2004; Lin and Spradling, 1995; Roper and Brown, 2004); however, based on our analysis of several fusome markers, we did not detect a

prominent fusome-like structure in zebrafish germline cysts. This finding suggests zebrafish GlCs may be more similar to the mouse GlCs, which also lack a prominent or stable fusome (Pepling and Spradling, 1998).

Additionally, we show that while asymmetries in the cytoskeleton and mitochondrial distribution in oogonia are evident, they do not depend on Buc. Finally, our analysis of centrosomes suggests that they are positioned near cytoplasmic bridges, consistent with ultrastructural analysis of zebrafish cysts (Marlow and Mullins, 2008). Taken together, these results suggest that the centrosome coordinates microtubule organization along the plane of cell division during cyst development. Although we observe decreased signal intensity of dynamic microtubules in *buc* mutants and *cbuc* transgenics, this network of microtubules is still sufficient for oogonial division, differentiation into oocytes, and meiotic progression.

The centrosome foreshadows early asymmetric Buc localization even when meiosis is disrupted

We found that Buc protein colocalizes with the centrosome in zygotene stage oocytes before Bb formation although we cannot distinguish whether the centrosome marks an initial pre-Bb site to which Buc is recruited, or if the centrosome is repolarized as occurs in *Drosophila* (Huynh and St Johnston, 2004) to the site of asymmetric Buc. Either way, this association is consistent with observations in other organisms that nuage and future Bb components organize around the oogonial centrosome (Huynh and St Johnston, 2004; Kloc et al., 2004; Sathananthan et al., 2000). Examination of *cbuc* transgenic and *magellan* mutant oocytes indicates that Buc colocalization with the centrosome is essential for oocyte polarization, but that other mechanisms including Bb translocation contribute at later stages.

During meiosis, the centrosomes coordinate chromosomal rearrangements associated with the leptotene-zygotene transition during prophase I (Scherthan et al., 2000). Previous work showed that meiosis can proceed independent of *buc* function and cellular polarization (Marlow and Mullins, 2008), but whether meiosis was required to generate asymmetric Buc was unknown. Our observation that Buc asymmetry is established before leptotene/zygotene transition in *vasa* mutants, which disrupt meiosis,

indicates that, as in yeast (Trelles-Sticken et al., 1999) and plants(Cowan et al., 2002), cellular polarity can be established independent of meiotic progression in zebrafish oocytes. Notably, accumulation of Buc in *vasa* mutant oogonia indicates that there are cellular mechanisms that coordinate the timing of cellular polarization and meiosis. Our findings are consistent with a model whereby coordination is achieved via interaction with the centrosome, with *vasa* directly or indirectly inhibiting Buc accumulation at the centrosome until meiotic entry (Figure 10).

Buc promotes the accumulation of microtubule filaments in primary oocyte

MFs are important for establishing and maintaining asymmetries in later stage oocytes of *Xenopus* and *Drosophila* (Messitt et al., 2008; Palacios and St Johnston, 2002; Robb et al., 1996; Yoon and Mowry, 2004). In zebrafish *magellan* mutants, which disrupt Spektraplakin/Macf1/Acf7, impaired microtubule organization is associated with failed Bb translocation, and thus failed maintenance of animal-vegetal polarity (Bontems et al., 2011; Gupta et al., 2010). In *Drosophila*, a *Macf1/shot* mutant has earlier defects in the maintenance of polarized microtubules associated with the fusome in the GIC, and consequently *shot* mutant GICs fail to specify the oocyte and arrest (Roper and Brown, 2004).

Our observations that Buc localizes to the centrosome and that both dynamic and stable microtubules are sparse in *buc* mutants suggests that Buc promotes microtubule-nucleating activity of the centrosome. The reduced density of acetylated microtubules in *buc* mutants at later stages could be explained by impaired transport or interactions between Buc and components of the microtubule cytoskeleton, like Kinesin motors (Campbell et al., 2015) to influence microtubule organization.

Finally, our observation that EB3 foci first localized near the centrosome and Buc domain opens up new areas of investigation to understand the function of these microtubule-based cage-like structures during Bb development. While it is unclear why there are two EB3 foci per oocyte, their localization near the centrosome at the periphery of the crescent-shaped asymmetric Buc suggests these microtubule-based structures may restrict the size of the Buc domain until the requisite Bb components, possibly endoplasmic reticulum, have aggregated. Once the Bb detaches from the

nucleus, the EB3 foci travel away from the nucleus and their apparent trajectory creates a “wedge-shape” that is reminiscent of the “wedge-shaped” distribution of RNAs that forms in the vegetal cortex of *Xenopus* oocytes (Forristall et al., 1995; Kloc and Etkin, 1995). Similarly in zebrafish, several germ plasm RNAs also exhibit a wedge-shape distribution in the vegetal-region of stage I oocytes (Bally-Cuif et al., 1998; Gupta et al., 2010; Kosaka et al., 2007; Marlow and Mullins, 2008). In *Xenopus*, RNAs enriched within the wedge domain, such as *Vg1*, are transported to the vegetal cortex via a mechanism that involves microtubules and kinesin motor proteins (reviewed in (Gagnon and Mowry, 2011)]. Therefore, this arrangement could be required for RNA entrapment and translocation. Moreover, previous work has shown that similar acentriolar EB1 foci that mark growing microtubule ends push the nucleus from the posterior pole to the dorsal anterior corner in *Drosophila* oocytes (Zimyanin et al., 2008). This raises the interesting possibility that growing microtubules are generating the force underlying Bb translocation from the nuclear periphery toward the oocyte cortex. Because these foci persist in stages after centriole elimination or disassembly, they are likely coordinated by a new organizing center in the oocyte, potentially the Bb. In support of this notion, these growing microtubule centers fail to form properly in *buc* mutants, which lack Bbs, and in *cbuc* transgenics, which form microtubules that fail to align with the centrosome, but are present in *mgn* mutants, which lack Bbs. Thus, these foci are Buc dependent. Interestingly, in *mgn* mutants, the localization of the EB3 centers is comparable to WT during stages when the centrosome is present, suggesting that initial coordination occurs normally. In contrast at later stages once the centrosome is lost and the Buc domain has translocated from the nucleus, the distance between EB3 foci is greater in *mgn* mutants compared to WT, indicating that coordination of these EB3 centers relies on Buc and possibly other cues from Bb.

Materials and Methods

Animals. AB strain wild-type, *buc*$^{p43/p43}$ (Bontems et al., 2009), *buc*$^{p106/p106}$ (Dosch et al., 2004), *mgn*$^{p6cv/p6cv}$ (Dosch et al., 2004), and *vasa*$^{sa6158/6158}$ (Hartung et al., 2014) zebrafish embryos were obtained from pairwise matings and reared according to standard procedure (Westerfield, 2000). Ovaries were obtained from 30 dpf >2.5 mo[illegible] female zebrafish except where indicated. All procedures and experimental protocols were in accordance with NIH guidelines and approved by Einste[illegible] and [illegible] Davis IACUCs.

Genotyping. Genomic DNA was isolated from fins. Genotyping of the *buc*^{p10} allele was performed as in (Bontems et al., 2009). Genotying of the *buc*^{43} allele was performed using dCAPS primers (p43dcapsRsaIF 5' TTGGC[illegible]GCTTATTC[illegible]TACAGGTA 3' and bucHRMAF 5' 5' TGGAGGAGAGCTCATCTAT[illegible]G 3') to amplify the region followed by digestion with RsaI, which generates a smaller product in WT. Genotyping of *mgn*^{p6cv} was performed as described in (Gupt[illegible]t al., 201[illegible] Genotyping of the *vasa*^{sa6158} was performed as described in (Hartung et a[illegible] 201[illegible]

Generation of Transgenic Li[illegible] The g[illegible] cell-expressed membrane-localized EGFP transgene was assembled from th[illegible] follow[illegible]g plasmids using GateWay cloning: p5E-*ziwi* promoter (Leu and Dr[illegible]er, 2010), p[illegible]E-egfpcaax (Kwan et al., 2007) and the multi-site destination ve[illegible]or pDest[illegible]l2pA (Villefranc et al., 2007)[reviewed in (Kawakami, 2005)]. The re[illegible]ting [illegible]asmid was designated pBD196. The resulting stable transgenic line produc[illegible] using this c[illegible]struct was designated Tg(*ziwi:egfpcaax*)^{uc11}.

[illegible]he EB3[illegible]Cherry transgene was generated using gateway cloning. Human EB3 coding [illegible]q[illegible]nce wa[illegible] amplified from pCS2+ EB3-GFP (Norden et al., 2009) using [illegible]B3[illegible]TG [illegible] (5'[illegible]TGGCCGTCAATGTGTACTC-3') and EB3_no_stop (5'-GTA[illegible]TCGTCC[illegible]GGTCTTCTT-3') primers, gel purified (28704, QIAGEN), and cloned [illegible] pCR8/GW/TOPO (K250020, Invitrogen) to generate pME-EB3. pME-EB3, p5E-ziwi pr[illegible]oter (Leu and Draper, 2010), and p3E-mCherry (Villefranc et al., 2007) were recombined into multi-site destination vector pDestTol2CG/CG2 (Kwan et al., 2007). The resulting transgenic line was designated Tg[ziwi:EB3-mCherry;cmlc2:eGFP].

Histology. Females or males were anesthetized in Tricaine as described (Westerfield, 2000). Ovaries were dissected and fixed in 4% paraformaldehyde overnight at 4ºC. Fixed ovaries were embedded in paraffin, sectioned, H&E stained, and imaged as in (Heim et al., 2014). Oocytes were staged according to (Selman et al., 1993).

Immunofluorescence. For F-actin labeling, dissected gonads were fixed for 4 hrs at 4°C in 3.7% formaldehyde in Actin Stabilizing Buffer (ASB) as in (Becker and Hartenstein, 1999) and staining was performed as described in (Topczewski and Sepich-Kimmel, 1999). For tubulin and EB3-mCherry immunofluorescence, tissues were fixed according to (Gard, 1991) and stained as in (Li-Villarreal et al., 2015). For BucN (Heim et al. 2014) and Spectrin (Millipore, MAB1622) staining, tissues were fixed overnight at 4°C in 4% PFA/1X PBS and then stained as described in (Li-Villarreal et al., 2015).

Image acquisition, processing and quantification. Fluorescence images were acquired with a Zeiss Axioobserver Apotome or a Leica SP2 point scanning microscope. Early meiotic oocytes were staged according to nuclear morphology (Leu and Draper, 2010). Oocytes were further categorized based on size. Quantification of Acetylated Tubulin staining intensity was performed as described in (Li-Villarreal et al., 2015). Quantification of α-Tubulin staining intensity was performed on maximal z-projections in ImageJ by manually tracing oocytes and measuring the pixel intensity within the selected region of interest. Further analysis of α-tubulin stained was performed on maximal z-projections to sort cystocytes into two classes based on the α-tubulin localization. Individual cells were bisected randomly or using the apparent asymmetric staining. For each half of the cell, the distance between the plasma membrane and the edge of the nucleus was measured in ImageJ. Cells were categorized as class I if the larger distance was >4 times that of the smaller distance. All other cells were categorized as class II. Images of EB3-mCherry transgenics were smoothed using ImageJ to reduce pixilation. Spatial measurements for EB3-mCherry foci were done using ImageJ software on maximal z-projections.

TEM. Samples were fixed with 2.5% glutaraldehyde, 2% paraformaldehyde in 0.1 M sodium cacodylate buffer. Samples were then processed by the Einstein Analytical Imaging Facility by postfixation with 1% osmium tetroxide followed by 2% uranyl acetate, dehydration through a graded series of ethanol and embedment in LX112 resin (LADD Research Industries, Burlington VT). Ultrathin sections (80 nm) were cut on a Leica EMUC7 ultramicrotome, stained with uranyl acetate followed by lead citrate and viewed on a JEOL 1200EX TEM at 80 kV at a magnification of 2000x to 20,000x. Three ovaries for each genotype were analyzed.

Analysis of mitochondria from TEM sections. Quantification was performed on cystocytes with readily apparent cell membranes where nuclear area was comparable (between 45 μm^2 and 60 μm^2). Mitochondria >0.25 μm^2 were counted manually.

Statistical analysis. GraphPad Prism 6 was used for statistical analysis. Error bars represent ±SEM unless otherwise stated. p values were determined by either two-tailed unpaired Student's t test to compare two populations or two-way ANOVA followed by a Tukey multiple comparisons test.

Author Contributions

Experiments were conceived and designed by M.M.F and F.L.M and performed by M.M.F. B.W.D generated the Tg(*Ziwi:egfpcaax*)^{uc11}line. M.M.F and F.L.M. interpreted data and wrote the manuscript with input from B.W.D.

Acknowledgements

This work was supported by NIH R01GM089979. T32-GM007491 supported MMF. NSF IOS #09296376 supported BWD. We thank Marlow lab members, our animal staff, and the AIF (NCI P30CA013330) and LSK for the EB3 vector. We thank OHK for comments.

References

al-Mukhtar, K.A., Webb, A.C., 1971. An ultrastructural study of primordial germ cells, oogonia and early oocytes in Xenopus laevis. J Embryol Exp Morphol 26, 195-217.

Bally-Cuif, L., Schatz, W.J., Ho, R.K., 1998. Characterization of the zebrafish Orb/CPEB-related RNA binding protein and localization of maternal components in the zebrafish oocyte. Mech Dev 77, 31-47.

Becker, K.A., Hart, N.H., 1999. Reorganization of filamentous actin and myosin-II in zebrafish eggs correlates temporally and spatially with cortical granule exocytosis. Journal of Cell Science 112, 97-110.

Bontems, F., Baerlocher, L., Mehenni, S., Bahechar, I., Farinelli, L., Dosch, R., 2011. Efficient mutation identification in zebrafish by microarray capturing and next generation sequencing. Biochem Biophys Res Commun 405, 373-376.

Bontems, F., Stein, A., Marlow, F., Lyautey, J., Gupta, T., Mullins, M.C., Dosch, R., 2009. Bucky ball organizes germ plasm assembly in zebrafish. Curr Biol 19, 414-422.

Campbell, P.D., Heim, A.E., Smith, M.Z., Marlow, F.L., 2015. Kinesin-1 interacts with Bucky ball to form germ cells and is required to pattern the zebrafish body axis. Development 142, 2996-3008.

Carrera, P., Johnstone, O., Nakamura, A., Casanova, J., Jackle, H., Lasko, P., 2000. VASA mediates translation through interaction with a Drosophila yIF2 homolog. Mol Cell 5, 181-187.

Cowan, C.R., Carlton, P.M., Cande, W.Z., 2001. The polar arrangement of telomeres in interphase and meiosis. Rabl organization and the bouquet. Plant Physiol 125, 532-538.

Cowan, C.R., Carlton, P.M., Cande, W.Z., 2002. Reorganization and polarization of the meiotic bouquet-stage cell can be uncoupled from telomere clustering. J Cell Sci 115, 3757-3766.

Cox, R.T., Spradling, A.C., 2003. A Balbiani body and the fusome mediate mitochondrial inheritance during Drosophila oogenesis. Development 130, 1579-1590.

de Cuevas, M., Lilly, M.A., Spradling, A.C., 1997. Germline cyst formation in Drosophila. Annu Rev Genet 31, 405-426.

de Cuevas, M., Spradling, A.C., 1998. Morphogenesis of the Drosophila fusome and its implications for oocyte specification. Development 125, 2781-2789.

Deng, W., Lin, H., 1997. Spectrosomes and fusomes anchor mitotic spindles during asymmetric germ cell divisions and facilitate the formation of a polarized microtubule array for oocyte specification in Drosophila. Dev Biol 189, 79-94.

Dosch, R., Wagner, D.S., Mintzer, K.A., Runke, G., Wiemelt, A.P., Mullins, M.C., 2004. Maternal control of vertebrate development before the midblastula transition: mutants from the zebrafish I. Dev Cell 6, 771-780.

Draper, B.W., 2012. Identification of oocyte progenitor cells in the zebrafish ovary. Methods Mol Biol 917, 157-165.

Forristall, C., Pondel, M., Chen, L., King, M.L., 1995. Patterns of localization and cytoskeletal association of two vegetally localized RNAs, Vg1 and Xcat-2. Development 121, 201-208.

Gagnon, J.A., Mowry, K.L., 2011. Molecular motors: directing traffic during RNA localization. Crit Rev Biochem Mol Biol 46, 229-239.

Gard, D.L., 1991. Organization, nucleation, and acetylation of microtubules in Xenopus laevis oocytes: a study by confocal immunofluorescence microscopy. Dev Biol 143, 346-362.

Gard, D.L., Affleck, D., Error, B.M., 1995. Microtubule organization, acetylation, and nucleation in Xenopus laevis oocytes: II. A developmental transition in microtubule organization during early diplotene. Dev Biol 168, 189-201.
Ghabrial, A., Schupbach, T., 1999. Activation of a meiotic checkpoint regulates translation of Gurken during Drosophila oogenesis. Nat Cell Biol 1, 354-357.
Gondos, B., 1973. Germ cell degeneration and intercellular bridges in the human fetal ovary. Z Zellforsch Mikrosk Anat 138, 23-30.
Gonzalez-Reyes, A., Elliott, H., St Johnston, D., 1995. Polarization of both major body axes in Drosophila by gurken-torpedo signalling. Nature 375, 654-658.
Grieder, N.C., de Cuevas, M., Spradling, A.C., 2000. The fusome organizes the microtubule network during oocyte differentiation in Drosophila. Development 127, 4253-4264.
Gupta, T., Marlow, F.L., Ferriola, D., Mackiewicz, K., Dapprich, J., Monos, D., Mullins, M.C., 2010. Microtubule actin crosslinking factor 1 regulates the Balbiani body and animal-vegetal polarity of the zebrafish oocyte. PLoS Genet 6, e1001043.
Hartung, O., Forbes, M.M., Marlow, F.L., 2014. Zebrafish vasa is required for germ-cell differentiation and maintenance. Mol Reprod Dev 81, 946-961.
Heim, A.E., Hartung, O., Rothhamel, S., Ferreira, E., Jaffrey, A., Marlow, F.L., 2014. Oocyte polarity requires a Bucky ball-dependent feedback amplification loop. Development 141, 842-854.
Huynh, J.-R., 2006. Fusome as a Cell-Cell Communication Channel of Drosophila Ovarian Cyst, Cell-Cell Channels. Springer New York, pp. 217-235.
Huynh, J.-R., St Johnston, D., 2004. The origin of Asymmetry: Early Polarisation of the Drosophila Germline Cyst and Oocyte. Current Biology 14, R438-R449.
Januschke, J., Gervais, L., Gillet, L., Keryer, G., Bornens, M., Guichet, A., 2006. The centrosome-nucleus complex and microtubule organization in the Drosophila oocyte. Development 133, 129-139.
Johnstone, O., Deuring, R., Bock, R., Linder, P., Fuller, M.T., Lasko, P., 2005. Belle is a Drosophila DEAD-box protein required for viability and in the germ line. Dev Biol 277, 92-101.
Johnstone, O., Lasko, P., 2004. Interaction with eIF5B is essential for Vasa function during development. Development 131, 4167-4178.
Kawakami, K., 2005. Transposon tools and methods in zebrafish. Dev Dyn 234, 244-254.
Kloc, M., Bilinski, S., Dougherty, M.T., Brey, E.M., Etkin, L.D., 2004. Formation, architecture and polarity of female germline cyst in Xenopus. Developmental Biology 266, 43-61.
Kloc, M., Etkin, L.D., 1995. Two distinct pathways for the localization of RNAs at the vegetal cortex in Xenopus oocytes. Development 121, 287-297.
Kloc, M., Jaglarz, M., Dougherty, M., Stewart, M.D., Nel-Themaat, L., Bilinski, S., 2008. Mouse early oocytes are transiently polar: three-dimensional and ultrastructural analysis. Exp Cell Res 314, 3243-3254.
Knaut, H., Pelegri, F., Bohmann, K., Schwarz, H., Nusslein-Volhard, C., 2000. Zebrafish vasa RNA but not its protein is a component of the germ plasm and segregates asymmetrically before germline specification. J Cell Biol 149, 875-888.
Komarova, Y., Lansbergen, G., Galjart, N., Grosveld, F., Borisy, G.G., Akhmanova, A., 2005. EB1 and EB3 control CLIP dissociation from the ends of growing microtubules. Mol Biol Cell 16, 5334-5345.

Kosaka, K., Kawakami, K., Sakamoto, H., Inoue, K., 2007. Spatiotemporal localization of germ plasm RNAs during zebrafish oogenesis. Mech Dev 124, 279-289.
Kuramochi-Miyagawa, S., Watanabe, T., Gotoh, K., Takamatsu, K., Chuma, S., Kojima-Kita, K., Shiromoto, Y., Asada, N., Toyoda, A., Fujiyama, A., Totoki, Y., Shibata, T., Kimura, T., Nakatsuji, N., Noce, T., Sasaki, H., Nakano, T., 2010. MVH in piRNA processing and gene silencing of retrotransposons. Genes Dev 24, 887-892.
Kwan, K.M., Fujimoto, E., Grabher, C., Mangum, B.D., Hardy, M.E., Campbell, D.S., Parant, J.M., Yost, H.J., Kanki, J.P., Chien, C.B., 2007. The Tol2kit: a multisite gateway-based construction kit for Tol2 transposon transgenesis constructs. Dev Dyn 236, 3088-3099.
Leu, D.H., Draper, B.W., 2010. The ziwi promoter drives germline-specific gene expression in zebrafish. Dev Dyn 239, 2714-2721.
Li-Villarreal, N., Forbes, M.M., Loza, A.J., Chen, J., Ma, T., Helde, K.A., Moens, C.B., Shin, J., Sawada, A., Hindes, A.E., Dubrulle, J., Schier, A.F., Longmore, G.D., Marlow, F.L., Solnica-Krezel, L., 2015. Dachsous1b cadherin regulates actin and microtubule cytoskeletal organization during early zebrafish embryogenesis. Development 142, 2704-2718.
Lim, A.K., Lorthongpanich, C., Chew, T.G., Tan, C.W., Shue, Y.T., Balu, S., Gounko, N., Kuramochi-Miyagawa, S., Matzuk, M.M., Chuma, S., Mahadevaiah, S.K., Schmidt, D.M., Solter, D., Knowles, B.B., 2013. The nuage mediates retrotransposon silencing in mouse primordial ovarian follicles. Development 140, 3819-3825.
Lin, H., Spradling, A.C., 1995. Fusome asymmetry and oocyte determination in Drosophila. Dev Genet 16, 6-12.
Lin, H., Yue, L., Spradling, A.C., 1994. The Drosophila fusome, a germline-specific organelle, contains membrane skeletal proteins and functions in cyst formation. Development 120, 947-956.
Linder, P., 2003. Yeast RNA helicases of the DEAD-box family involved in translation initiation. Biol Cell 95, 157-167.
Maack, G., Segner, H., 2003. Morphological development of the gonads in zebrafish. Journal of Fish Biology 62, 895-906.
Mahowald, A.P., Strassheim, J.M., 1970. Intercellular migration of centrioles in the germarium of Drosophila melanogaster. An electron microscopic study. J Cell Biol 45, 306-320.
Marlow, F.L., Mullins, M.C., 2008. Bucky ball functions in Balbiani body assembly and animal-vegetal polarity in the oocyte and follicle cell layer in zebrafish. Dev Biol 321, 40-50.
Megraw, T.L., Kaufman, T.C., 2000. The centrosome in Drosophila oocyte development. Curr Top Dev Biol 49, 385-407.
Messitt, T.J., Gagnon, J.A., Kreiling, J.A., Pratt, C.A., Yoon, Y.J., Mowry, K.L., 2008. Multiple kinesin motors coordinate cytoplasmic RNA transport on a subpopulation of microtubules in Xenopus oocytes. Dev Cell 15, 426-436.
Nakagawa, H., Koyama, K., Murata, Y., Morito, M., Akiyama, T., Nakamura, Y., 2000. EB3, a novel member of the EB1 family preferentially expressed in the central nervous system, binds to a CNS-specific APC homologue. Oncogene 19, 210-216.
Nakamura, S., Kobayashi, K., Nishimura, T., Higashijima, S., Tanaka, M., 2010. Identification of germline stem cells in the ovary of the teleost medaka. Science 328, 1561-1563.
Norden, C., Young, S., Link, B.A., Harris, W.A., 2009. Actomyosin Is the Main Driver of Interkinetic Nuclear Migration in the Retina. Cell 138, 1195-1208.

Palacios, I.M., St Johnston, D., 2002. Kinesin light chain-independent function of the Kinesin heavy chain in cytoplasmic streaming and posterior localisation in the Drosophila oocyte. Development 129, 5473-5485.
Pek, J.W., Kai, T., 2011. A role for vasa in regulating mitotic chromosome condensation in Drosophila. Curr Biol 21, 39-44.
Pepling, M.E., de Cuevas, M., Spradling, A.C., 1999. Germline cysts: a conserved phase of germ cell development? Trends Cell Biol 9, 257-262.
Pepling, M.E., Spradling, A.C., 1998. Female mouse germ cells form synchronously dividing cysts. Development 125, 3323-3328.
Robb, D.L., Heasman, J., Raats, J., Wylie, C., 1996. A kinesin-like protein is required for germ plasm aggregation in Xenopus. Cell 87, 823-831.
Roper, K., Brown, N.H., 2004. A spectraplakin is enriched on the fusome and organizes microtubules during oocyte specification in Drosophila. Curr Biol 14, 99-110.
Roth, S., Neuman-Silberberg, F.S., Barcelo, G., Schupbach, T., 1995. cornichon and the EGF receptor signaling process are necessary for both anterior-posterior and dorsal-ventral pattern formation in Drosophila. Cell 81, 967-978.
Saito, K., Sakai, C., Kawasaki, T., Sakai, N., 2014. Telomere distribution pattern and synapsis initiation during spermatogenesis in zebrafish. Dev Dyn 243, 1448-1456.
Sathananthan, A.H., Selvaraj, K., Trounson, A., 2000. Fine structure of human oogonia in the foetal ovary. Mol Cell Endocrinol 161, 3-8.
Scherthan, H., Jerratsch, M., Li, B., Smith, S., Hulten, M., Lock, T., de Lange, T., 2000. Mammalian meiotic telomeres: protein composition and redistribution in relation to nuclear pores. Mol Biol Cell 11, 4189-420
Selman, K., Wallace, R.A., Sarka, A., Qi, , 1993. Stages of oocyte development in the zebrafish, Brachydanio rerio. Journal of Morphology 218, 203-224.
Snapp, E.L., Iida, T., Frescas, D., Lippincott-Schwartz, J., Lilly, M.A., 2004. The fusome mediates intercellular endoplasmic reticulum connectivity in Drosophila ovarian cysts. Mol Biol Cell 15, 4512-452
Song, Y., Brady, S., 2015. Post-translational modifications of tubulin: pathways to functional diversity of microtubules. Trends Cell Biol 25, 125-136.
Stearns, T., Evans, L., Kirschner, M., 1991. Gamma-tubulin is a highly conserved component of the centrosome. Cell 65, 825-836.
Stepanova, T., Slemmer, J., Hoogenraad, C.C., Lansbergen, G., Dortland, B., De Zeeuw, C.I., Grosveld, F., van Cappellen, G., Akhmanova, A., Galjart, N., 2003. Visualization of microtubule growth in cultured neurons via the use of EB3-GFP (end-binding protein 3-green fluorescent protein). J Neurosci 23, 2655-2664.
Strasser, M.J., MacKenzie, N.C., Dumstrei, K., Nakkrasae, L.I., Stebler, J., Raz, E., 2008. Control over cell morphology and segregation of Zebrafish germ cell granules during embryonic development. BMC Dev Biol 8, 58.
Styhler, S., Nakamura, A., Swan, A., Suter, B., Lasko, P., 1998. vasa is required for GURKEN accumulation in the oocyte, and is involved in oocyte differentiation and germline cyst development. Development 125, 1569-1578.
Takahashi, H., 1977. Juvenile Hermaphroditism in the Zebrafish, Brachydanio rerio. Bull Fac Fish Hokkaido Univ 28, 57-65.

Tanaka, S.S., Toyooka, Y., Akasu, R., Katoh-Fukui, Y., Nakahara, Y., Suzuki, R., Yokoyama, M., Noce, T., 2000. The mouse homolog of Drosophila Vasa is required for the development of male germ cells. Genes Dev 14, 841-853.
Topczewski, J., Solnica-Krezel, L., 1999. Cytoskeletal dynamics of the zebrafish embryo. Methods Cell Biol 59, 205-226.
Trelles-Sticken, E., Loidl, J., Scherthan, H., 1999. Bouquet formation in budding yeast: initiation of recombination is not required for meiotic telomere clustering. J Cell Sci 112 (Pt 5), 651-658.
Villefranc, J.A., Amigo, J., Lawson, N.D., 2007. Gateway compatible vectors for analysis of gene function in the zebrafish. Dev Dyn 236, 3077-3087.
Wang, X.G., Bartfai, R., Sleptsova-Freidrich, I., Orban, L., 2007. The timing and extent of 'juvenile ovary' phase are highly variable during zebrafish testis differentiation. Journal of Fish Biology 70, 33-44.
Westerfield, M., 2000. The zebrafish book. A guide for the laboratory use of zebrafish (Danio rerio). Univ, of Oregon Press, Eugene.
Yajima, M., Wessel, G.M., 2011. The DEAD-box RNA helicase Vasa functions in embryonic mitotic progression in the sea urchin. Development 1 3217-2222.
Yamashita, Y.M., 2009. The centrosome and asymmetric cell division. Prion 3, 84-88.
Yoon, Y.J., Mowry, K.L., 2004. Xenopus Staufen is a component of a ribonucleoprotein complex containing Vg1 RNA and kinesin. Development 131, 3 35-3045.
Yoshida, M., Katsuyama, S., Tateho, K., Nakamura, J. Miyos , J., Ohba, T., Matsuhara, H., Miki, F., Okazaki, K., Haraguchi, T., Niwa Hiraoka, Y., amamoto, A., 2013. Microtubule-organizing center formation at telomere induces meiotic telomere clustering. J Cell Biol 200, 385-395.
Zhao, T., Graham, O.S., Rapos A., St Johnston, D., 2012. Growing microtubules push the oocyte nucleus to polarize the Drosophila dorsal-ventral axis. Science 336, 999-1003.

Figures

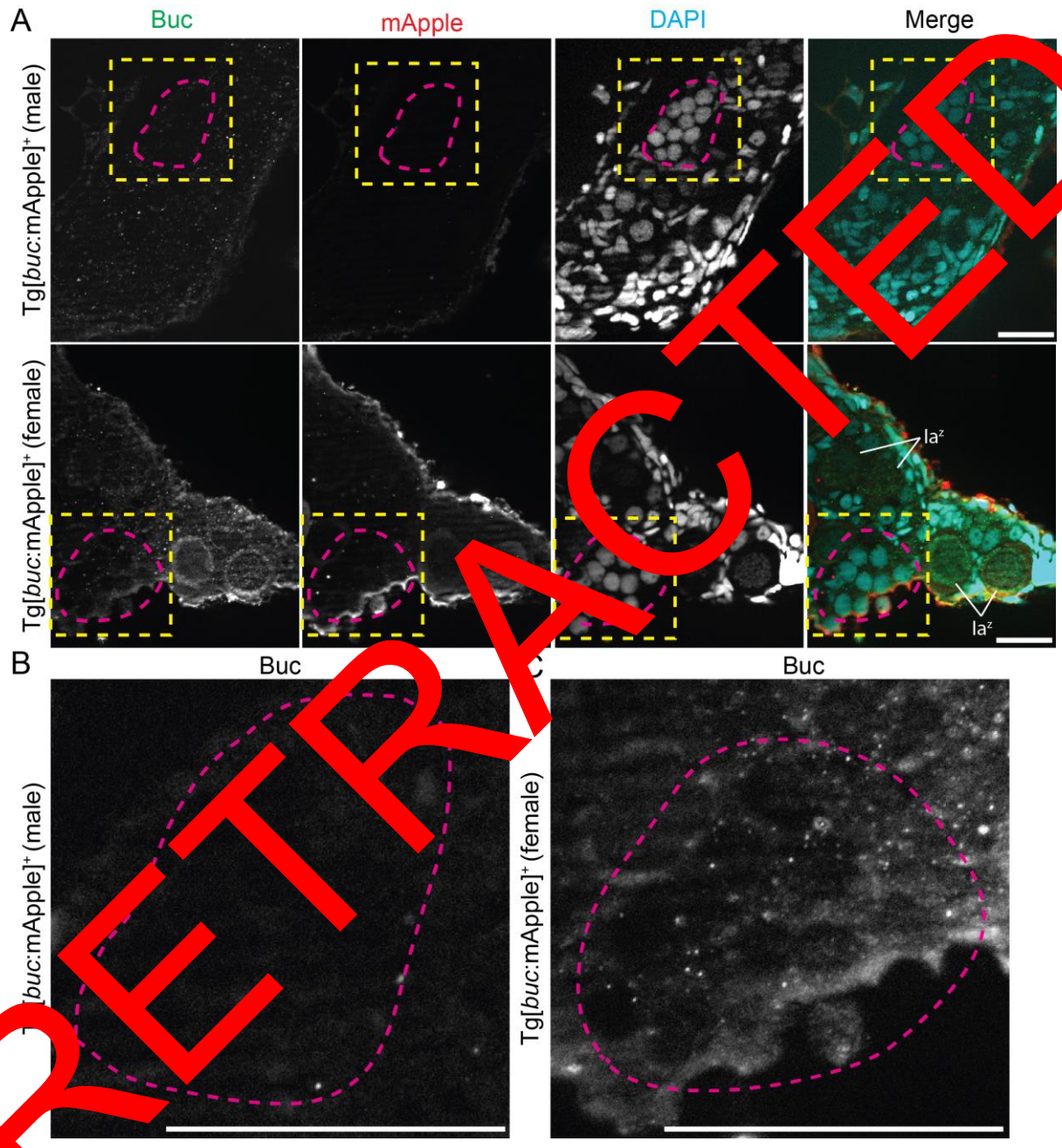

Figure 1. Endogenous Buc protein in female germline cysts. A) Endogenous Buc protein is detected in Tg[*buc*:mApple]$^{+}$, but not Tg[*buc*:mApple]$^{-}$ gonads. 5/14 fish examined that did not express mApple in the germ cells and had no detectable

endogenous Buc protein (juvenile gonad transitioning to a testis) and 9/14 fish that expressed mApple in the germ cells had detectable endogenous Buc protein (juvenile ovary). Dotted magenta line outlines a mid-stage germline cyst. Yellow dashed boxes indicate the zoomed in region of interest in panels B and C. B) Buc immunostained juvenile gonad transitioning to a testis. C) Buc immunostained juvenile ovary. Scale bars are 40 μm in panel A and 50 um in panels B&C.

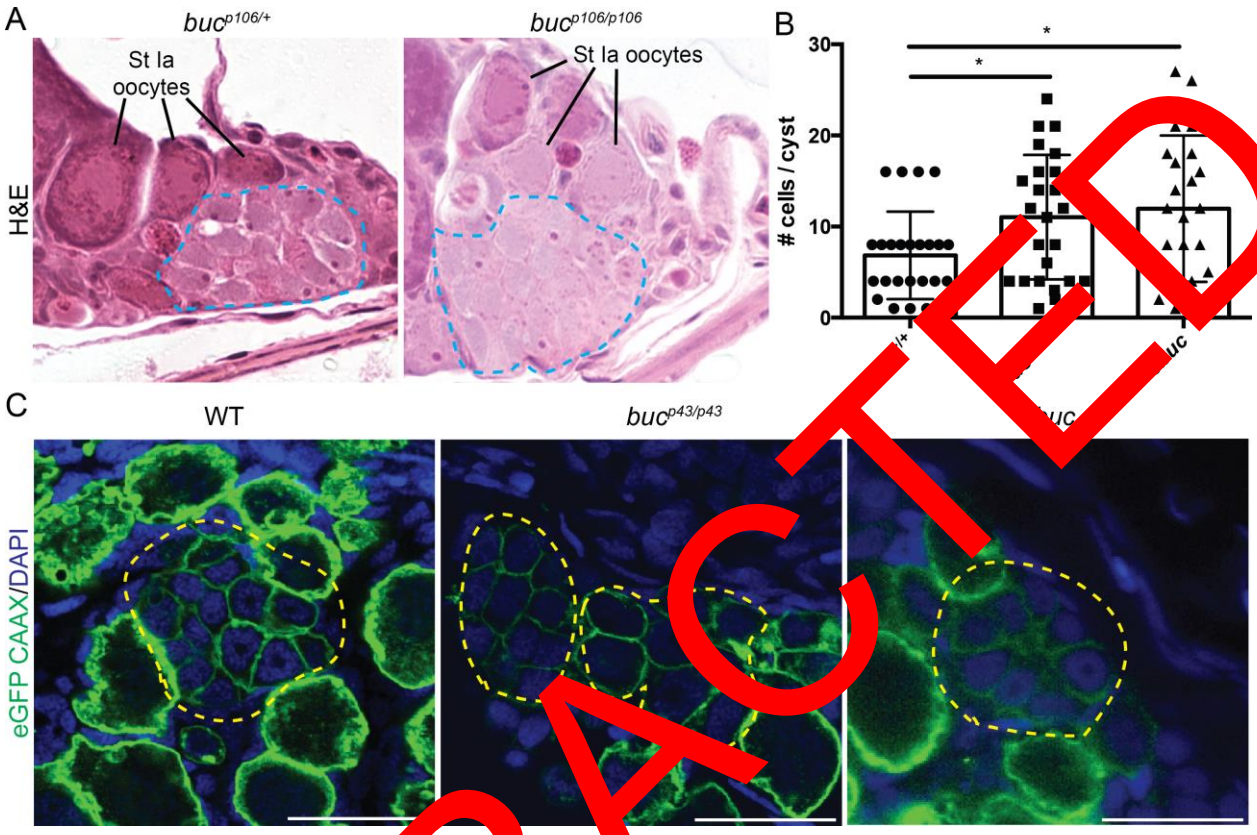

Figure 2. Buc regulates germline cyst development prior to Bb formation. A) H&E staining of *buc*$^{p106/+}$ and *buc*$^{p106/p106}$ juvenile gonads at 42 dpf. B) Quantification of germline cyst size from Tg[ziwi:eGFP-CAAX]/DAPI labeled gonads as shown in C. Error bars show mean±s.e.m., $p < 0.05$. C) Juvenile gonads of WT, *buc*$^{p43/p43}$ mutants and *cbuc* transgenics. Scale bars are 40 μm in panel C.

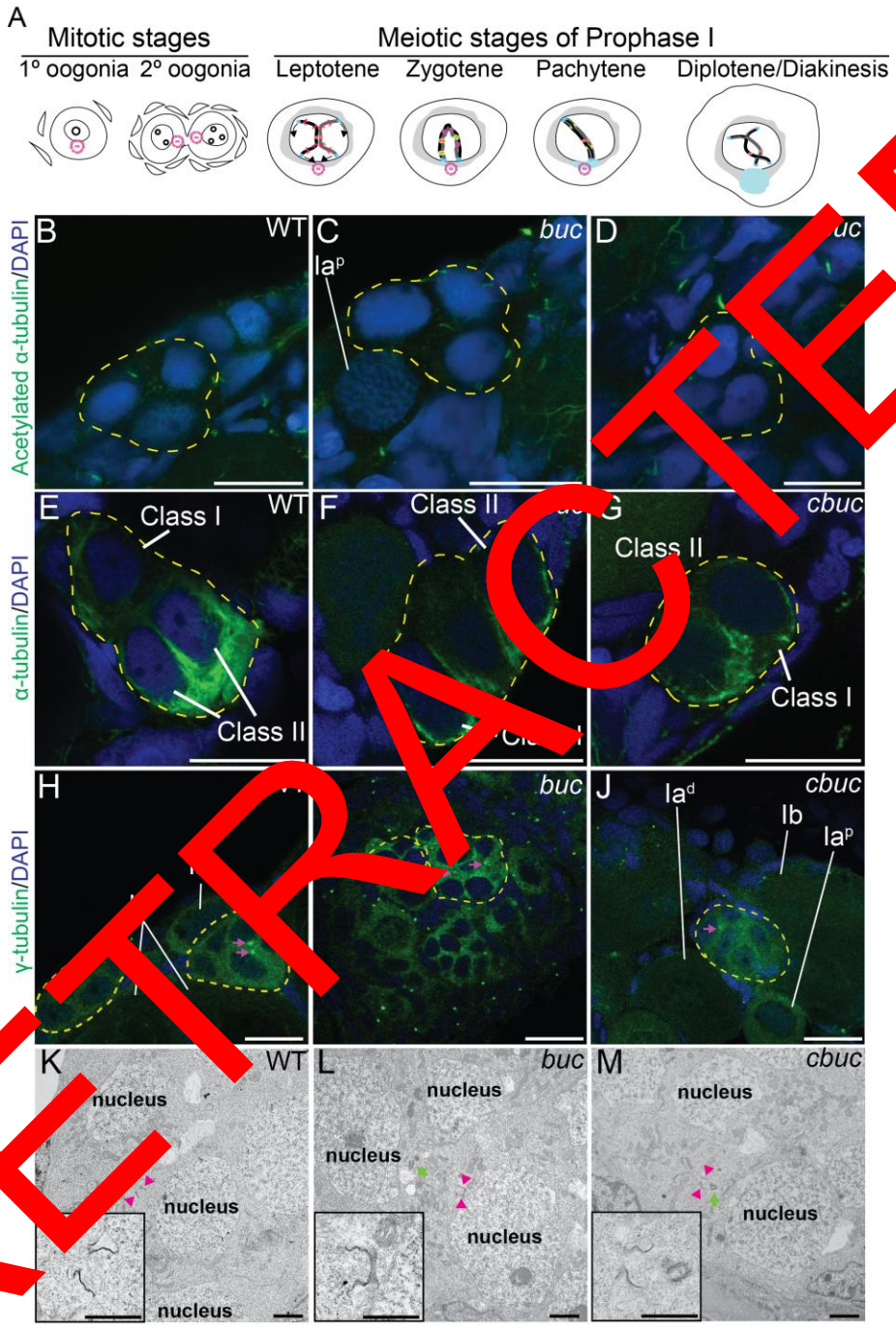

Figure 3. Microtubule cytoskeleton organization in mitotic oogonia is independent of *buc*. A) Schematic showing the development of mitotic oogonia (cystocytes) to early meiotic oocytes progressing through prophase I. Oogonia with a single prominent

nucleolus (circles in nucleus) were defined as primary, and those with multiple nucleoli were defined as secondary oogonia. The centrosome (magenta) is present from mitotic stages through pachytene stage. Asymmetric Buc protein expression domains in meiotic stages are indicated in light blue. B-D) Localization of stable microtubules labeled with Acetylated α-tubulin in cystocytes of WT, *buc*$^{p43/p43}$, and *cbuc* juvenile ovaries. E-G) Localization of dynamic microtubules labeled with α-tubulin in cystocytes of WT, *buc*$^{p43/p43}$, and *cbuc* juvenile ovaries. Class I cystocytes have a centrally positioned nucleus whereas Class II cystocytes have an asymmetrically positioned nucleus. H-J) Localization of γ-tubulin in cystocytes of WT, *buc*$^{p43/p43}$, and *cbuc* juvenile ovaries. Ia^{d} indicated diplotene and Ia^{p} indicates pachytene of prophase I, and Ib indicates Bb stage prophase I arrested oocyte. K-L) Ultrastructural analysis of WT, *buc*$^{p43/p43}$, and *cbuc* juvenile ovaries reveals that oogonial centrioles (pink arrows) occupy the cytoplasm that is proximal to the intercellular bridge (green arrow) in all genotypes examined. Insets show higher magnification images of the intercellular bridges. B-J) Individual cystocytes are outlined with yellow dashed lines. Scale bars for panels B-J are 25 μm. Scale bars for panels K-L are 2 μm and 1 μm for the insets. Data for fluorescently labeled samples is from 20-40 cystocytes from n>4 juvenile ovaries.

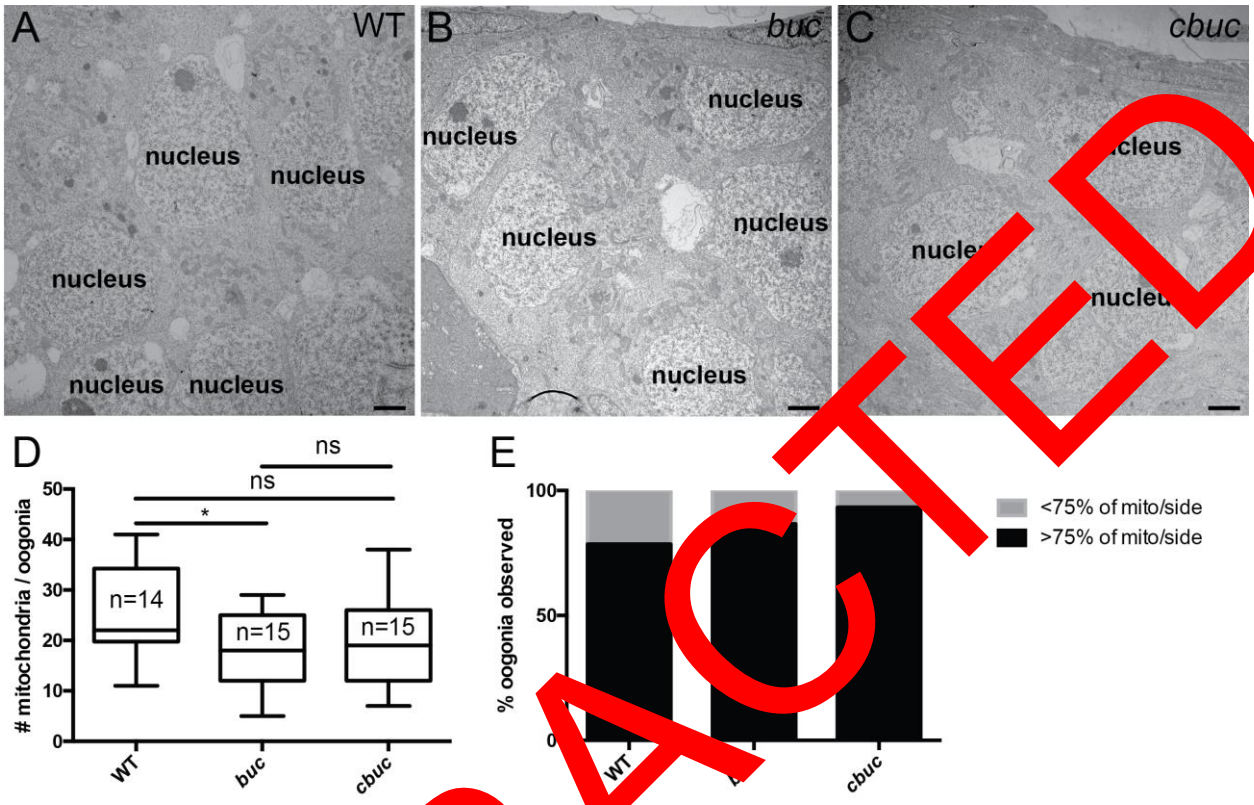

Figure 4. Mitochondrial distribution in mitotic oogonia is *buc* independent. A-C) 2000x TEM images of mitotic cysts from WT, *buc*$^{p43/p43}$, and *cbuc* juvenile ovaries. D) Quantification of total number of mitochondria >0.2 µm per cystocyte for each genotype. Box and whiskers plot shows the median and min to max data points, *p<.05. E) Quantification of the percentage of cystocytes observed for each category indicated. Black bar denotes asymmetric mitochondria distribution. All scale bars are 2 µm.

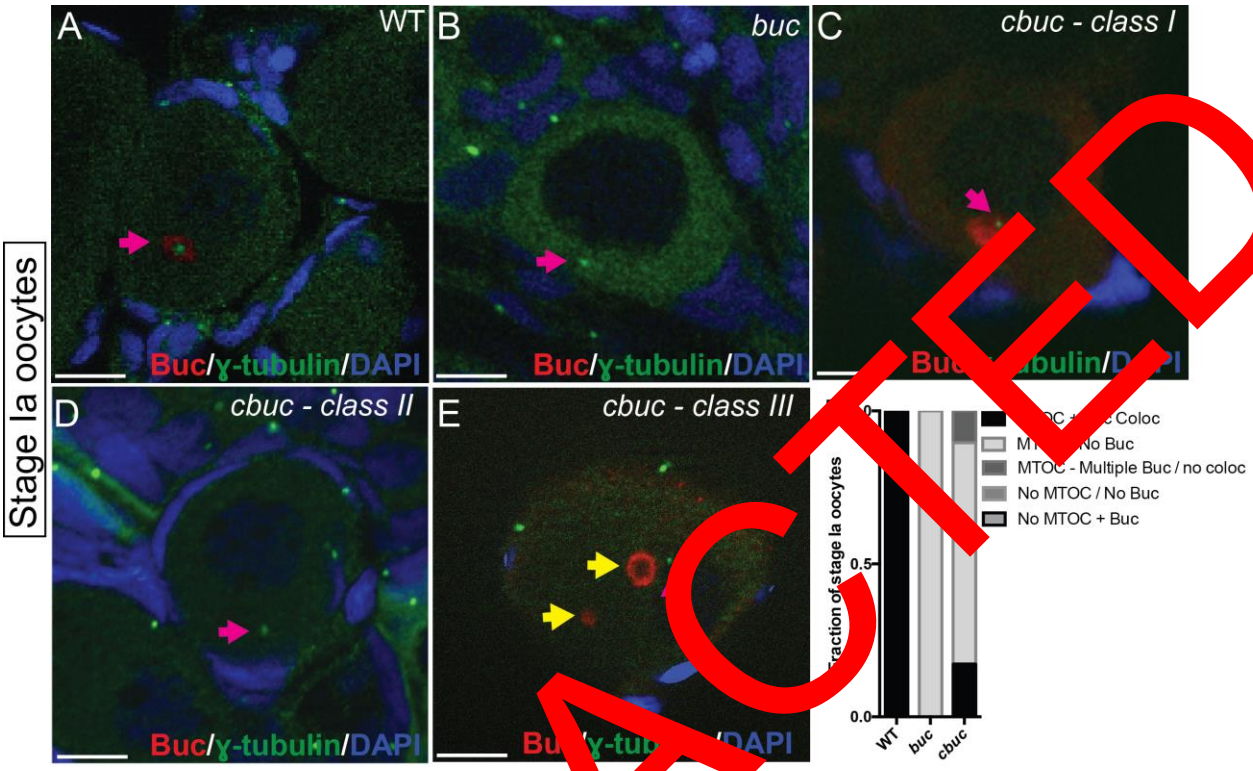

Figure 5. Buc colocalizes with the centrosome of Stage Ia oocytes. A-C,D,E) Centrosomes (microtubule organizing centers containing gamma-tubulin are indicated with pink arrows) are proximal to the nucleus in stage Ia oocytes (prophase I early Bb formation) of (A) WT and (B-E)polarity mutants. (C-E) Three classes are observed in *cbuc* ovaries. (C) oocytes that resemble WT, (D) oocytes that resemble *buc* mutants, and oocytes with multiple Buc domains that are not colocalized with the centrosome (yellow arrows). In (A) WT early asymmetric Buc protein colocalize with the centrosome. F) Quantification of γ-tubulin containing centrosomes and their relationship to Buc protein in WT, *buc*$^{p43/p43}$ mutants, and *cbuc* transgenic oocytes. Data from n>20 oocytes from 3 or more ovaries. Scale bars are 10 μm.

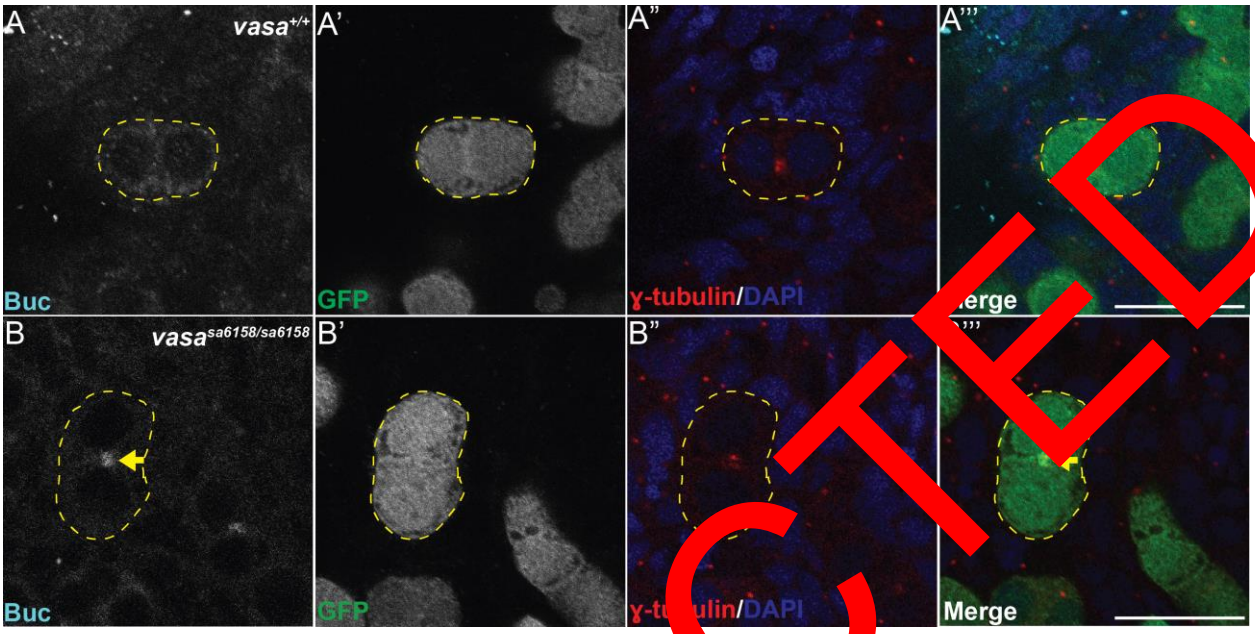

Figure 6. Buc localizes to the centrosome in mutants that disrupt meiosis

Buc and ɣ-tubulin immunostaining in WT and *vasa*$^{sa6158/sa6158}$ juvenile gonads at 28 dpf. A) In *vasa*$^{+/+}$ cystocytes, Buc protein is diffuse and not asymmetrically localized. B) Localization of Buc protein to the centrosome in *vasa*$^{sa6158/sa6158}$ cystocytes. A' and B') The Tg[ziwi:eGFP]$^{+}$ reporter marks the germ cells. Yellow dashed line outlines cystocytes. Yellow arrow points to asymmetric Buc protein in *vasa*$^{sa6158/sa6158}$ cystocytes. Scale bars are 25 µm.

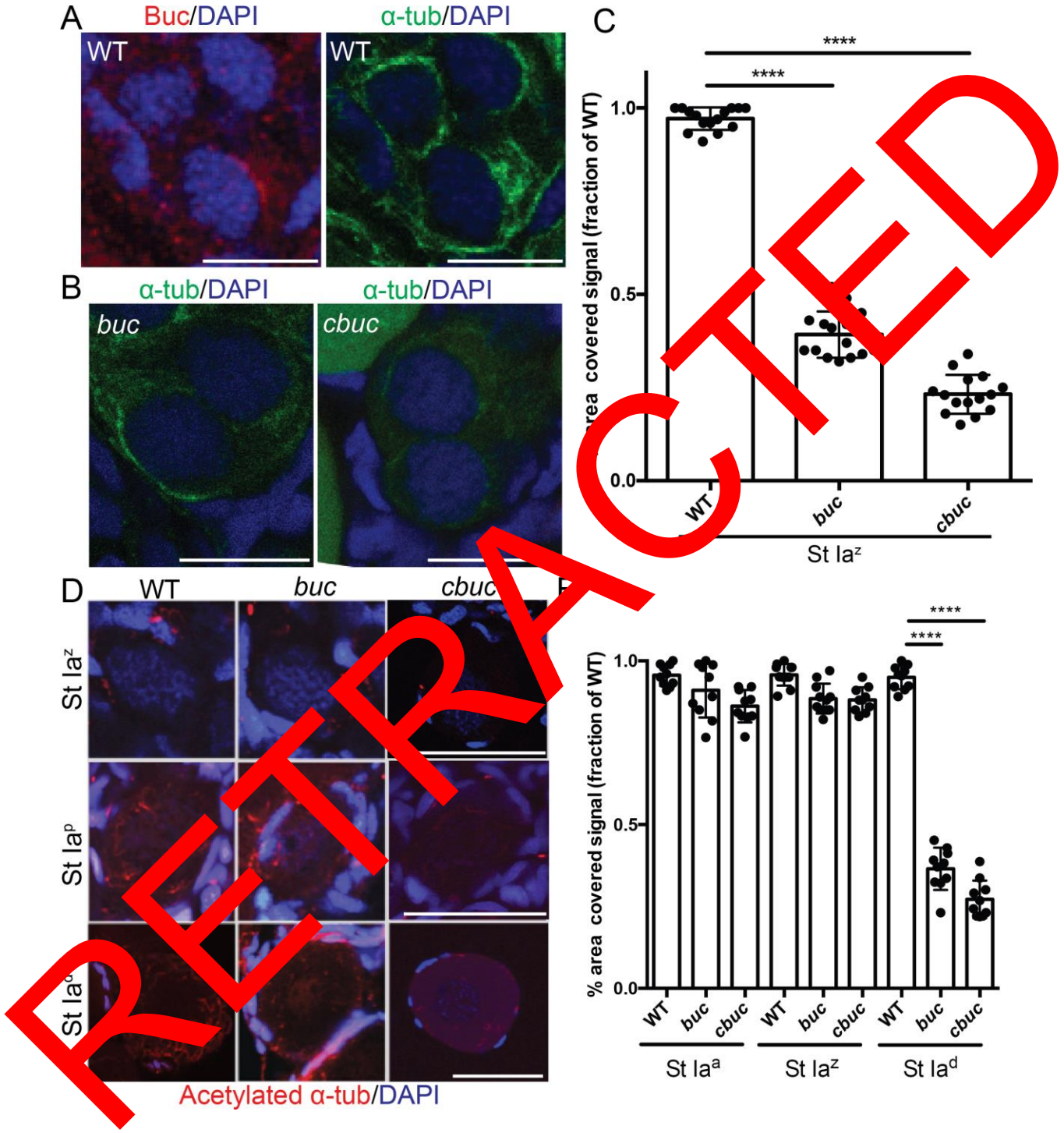

Figure 7. Microtubule filament density but not distribution depends on Buc prior to Balbiani body formation. A) Distribution of microtubule filaments and Buc protein in

WT St Ia^{z} (zygotene) oocytes. B) Distribution of microtubule filaments in *buc*$^{p43/p43}$ and *cbuc* oocytes. C) Quantification of α-tubulin signal coverage. Error bars show mean±s.e.m., ****p<.0001. D) Distribution of acetylated microtubules in wild-type, *buc*$^{p43/p43}$, and *cbuc* oocytes when the centrosome is present (zygotene (Ia^{z}) through pachytene (Ia^{p}), and after centrosome dispersal (diplotene (Ia^{d}) stage). E) Quantification of acetylated tubulin signal coverage. Error bars show mean±s.e.m., ****p<.0001. Scale bars are 25 μm in panels A and B and 20 μm in panel D.

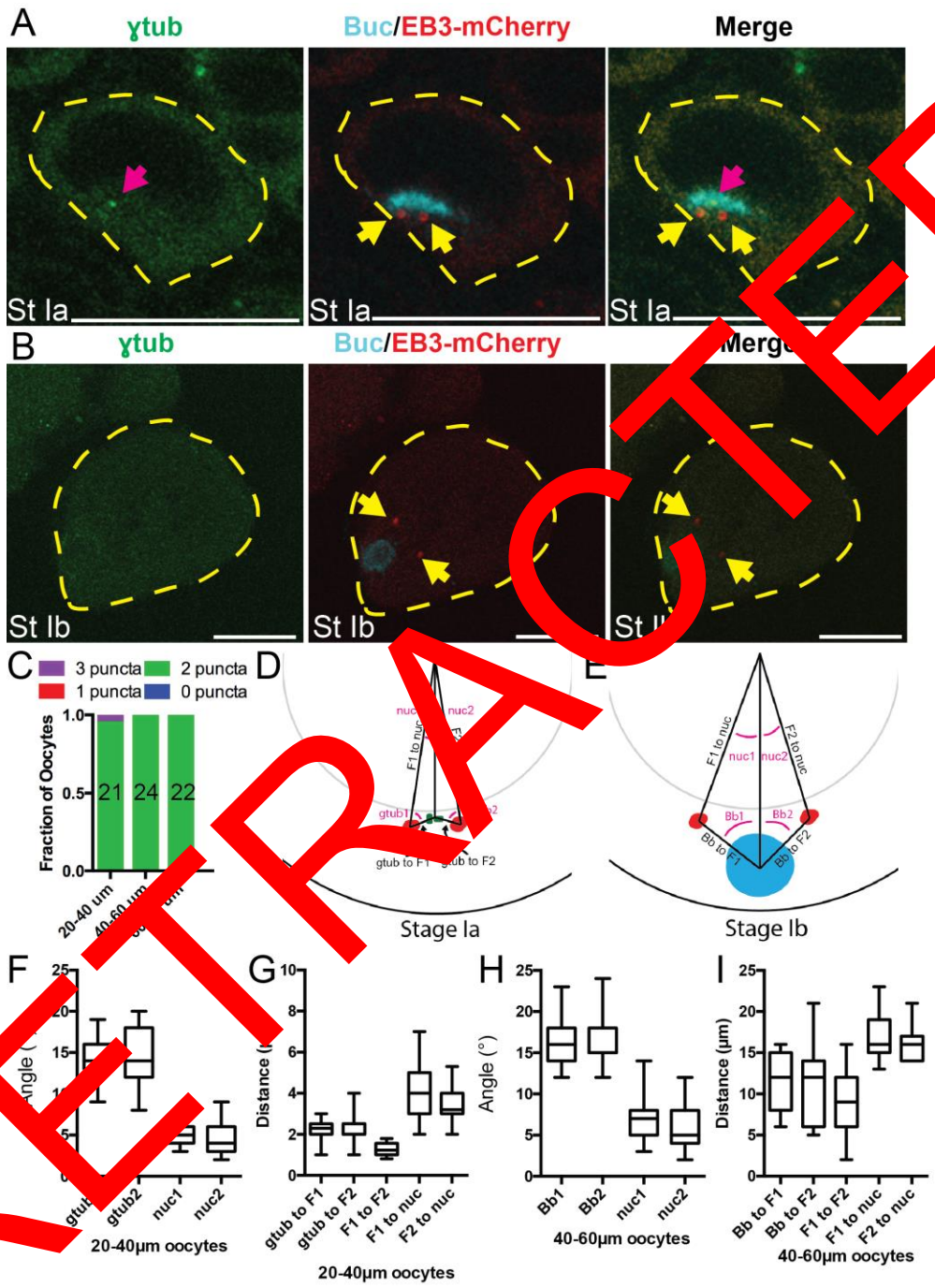

Figure 8. EB3-mCherry foci are proximal to the centrosome and Buc protein during Bb assembly. A) Localization of EB3-mCherry foci (yellow arrows) relative to endogenous Buc protein and ɣ-tubulin (pink arrows) in WT St Ia oocytes. B) Localization

of EB3-mCherry foci (yellow arrows) relative to Buc protein. C) Quantification of EB3-mCherry foci per oocyte. D) Schematic of a stage Ia oocyte showing the distances and angles measured in panels F and G. E) Schematic of a stage Ib oocyte showing the distances and angles measured in panels H and I. The gtub to F1 or F2 distance is the distance between the center of the γtub puncta and the EB3-mCherry foci F1 and F2, respectively. The Bb to F1 or F2 distance is the distance between the center of the Bb (Blue) and the EB3-mCherry foci F1 and F2, respectively. The F1 to F2 distance is the distance between the two EB3-mCherry foci. The F1 or F2 to nuc distance is the distance between the center of the nucleus and the EB3-mCherry foci F1 and F2, respectively. The gtub1 and gtub2 angles are created between the center of the γ-tub puncta and the EB3-mCherry foci F1 and F2, respectively. The nuc1 and nuc2 angles are created between the center of the nucleus and the EB3-mCherry foci F1 and F2, respectively. Scale bars are 25 μm.

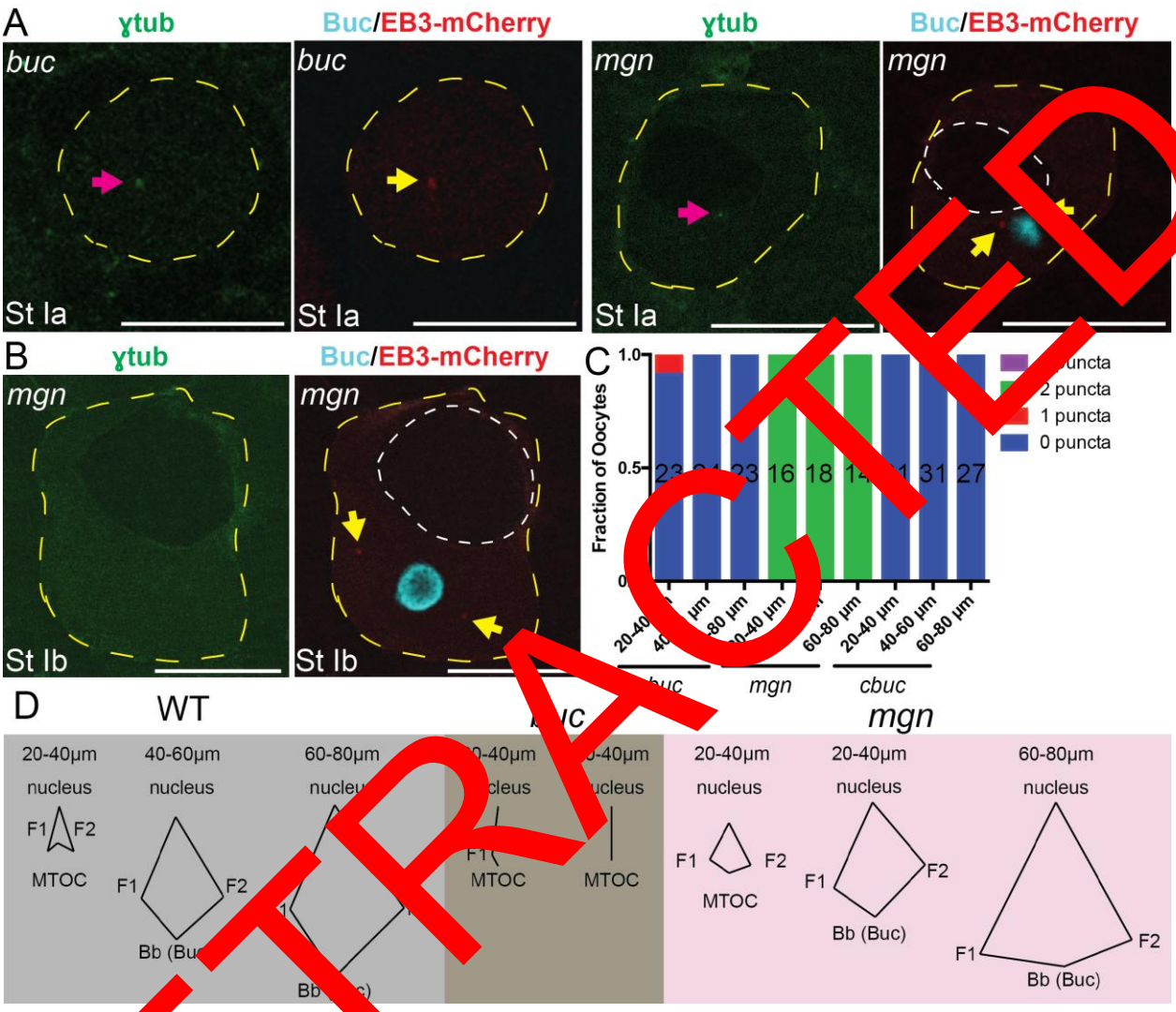

Figure [illegible] EB[illegible]-mCherry foci depend on Buc but not Macf1. A) Localization of EB3-m[illegible]rry foci (yel[illegible]w arrows) relative to endogenous Buc protein, γ-tubulin (pink arrow[illegible]), and D[illegible]PI in *buc*$^{p43/p43}$ and *mgn*$^{auie/auie}$ St Ia oocytes. B) Localization of EB3-m[illegible]herry foci (yellow arrows) relative to endogenous Buc protein, γ-tubulin, and DAPI in *m[illegible]*$^{auie/auie}$ St Ib oocytes. C) Quantification of EB3-mCherry per oocyte in WT and *buc* mutants. D) Representative polygons created from averaging the angles and distances between EB3 foci in WT, *buc*$^{p43/p43}$, and *mgn*$^{auie/auie}$ mutant oocytes. Scale bars are 25 μm. White dashed lines in panels A&B outline the nucleus of *mgn*$^{auie/auie}$ mutant oocytes.

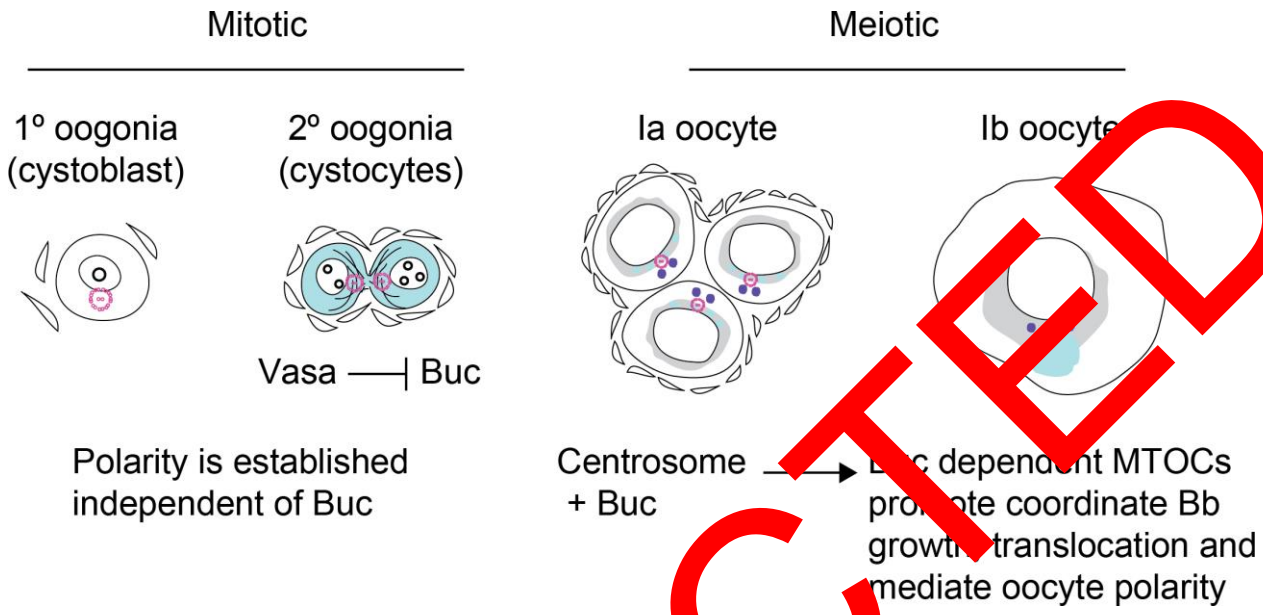

Figure 10. Buc alignment with the centrosome is required for proper oocyte polarization. Mitotic oogonia are polarized relative to the intracellular bridges. The centrosome (magenta) is adjacent to the intracellular bridges of mitotic oogonia and persists through pachytene stage of prophase I. Dynamic microtubules and mitochondria are also asymmetrically distributed in oogonia. In WT oogonia Buc protein (indicated in light blue) is present, but due to the activity of Vasa is not recruited to the centrosome until prophase I of meiosis. During the zygotene stage of prophase I, asymmetric Buc protein colocalizes with the centrosome and mediates the formation of meiotic MTOCs as well as microtubule-dependent cage-like structures, as revealed by the spatial arrangement of their plus-end tips (purple dots) in a Buc dependent manner. Colocalization of Buc protein with the centrosome is essential for normal Bb development and to generate a robust microtubule network that likely mediates Bb translocation and delivery of germ plasm and patterning molecules to the vegetal cortex.